JBC Papers in Press. Published on June 16, 2005 as Manuscript M504306200

# PLANT γ-GLUTAMYL HYDROLASES AND FOLATE POLYGLUTAMATES: CHARACTERIZATION, COMPARTMENTATION, AND CO-OCCURRENCE IN VACUOLES*

**Giuseppe Orsomando‡, Rocío Díaz de la Garza‡, Brian J. Green¶, Mingsheng Peng¶, Philip A. Rea¶, Thomas J. Ryan‖, Jesse F. Gregory III§, and Andrew D. Hanson‡**

*From the ‡Horticultural Sciences and §Food Science and Human Nutrition Departments, University of Florida, Gainesville, Florida 32611, the ¶Plant Science Institute, Department of Biology, University of Pennsylvania, 3800 Hamilton Walk, Philadelphia, Pennsylvania 19104, and the ‖Wadsworth Center, New York State Department of Health, Albany, New York 12201*

Running Title: Plant γ-Glutamyl Hydrolases and Folate Polyglutamates

**Address correspondence to: Andrew D. Hanson, Horticultural Sciences Dept., University of Florida, Gainesville, FL 32611. Tel. (352) 392-1928 x 334; Fax: (352) 392-5653; E-mail: adha@mail.ifas.ufl.edu

**γ-Glutamyl hydrolase (GGH, E.C. 3.4.19.9) catalyzes removal of the polyglutamyl tail from folyl and *p*-aminobenzoyl polyglutamates. Plants typically have one or a few GGH genes; *Arabidopsis* has three, tandemly arranged on chromosome 1, which encode proteins with predicted secretory pathway signal peptides. Two representative *Arabidopsis* GGH proteins, AtGGH1 and AtGGH2 (the At1g78660 and At1g78680 gene products, respectively) were expressed in truncated form in *Escherichia coli* and purified. Both enzymes were active as dimers, had low $K_m$ values (0.5 to 2 μM) for folyl and *p*-aminobenzoyl pentaglutamates, and acted as endopeptidases. However, despite 80% sequence identity, they differed in that AtGGH1 cleaved pentaglutamates mainly to di- and triglutamates, whereas AtGGH2 yielded mainly monoglutamates. Analysis of subcellular fractions of pea leaves and red beet roots established that GGH activity is confined to the vacuole and that this activity, if not so sequestered, would deglutamylate all cellular folylpolyglutamates within minutes. Purified pea leaf vacuoles contained an average of 20% of the total cellular folate, compared to ~50% and ~10%, respectively, in mitochondria and chloroplasts. The main vacuolar folate was 5-methyltetrahydrofolate, of which 51% was polyglutamylated. In contrast, the principal mitochondrial and chloroplastic forms were 5-formyl- and 5,10-methenyltetrahydrofolate polyglutamates, respectively. In beet roots, 16 to 60% of the folate was vacuolar, and was again mainly 5-methyltetrahydrofolate, of which 76% was polyglutamylated. These data point to a hitherto unsuspected role for vacuoles in folate storage. Furthermore, the paradoxical co-occurrence of GGH and folylpolyglutamates in vacuoles implies that the polyglutamates are somehow protected from GGH attack.**

In plants, as in other organisms, tetrahydrofolate (THF)[1] and its derivatives – collectively termed folates – usually have γ-linked polyglutamyl tails of up to about seven residues attached to the first glutamate (Fig. 1*A*) (1, 2). The tail critically affects the cofactor activity and transport of folates because most folate-dependent enzymes prefer polyglutamates while most carriers prefer monoglutamates (3, 4). By favoring protein binding, the tail also enhances folate stability since bound folate is less prone to oxidative degradation (1). The enzyme that adds the polyglutamyl tails, folylpolyglutamyl synthetase, has been well studied in plants and shown to have mitochondrial, plastidial, and cytosolic isoforms (5, 6). Less is known for plants about the enzyme that removes the tails, γ-glutamylhydrolase (GGH), although soluble GGH activity (5, 7) and GGH-like mRNAs (8, 9) clearly occur widely.

Biochemical characterization of plant GGHs has so far been limited to crude extracts (9, 10) or a mixture of isoforms (11) and has produced conflicting results on the enzyme's structure and mode of action. Furthermore, the subcellular location of plant GGH is unclear; cytosolic (11) or extracellular (12) sites have been proposed, but the vacuole is another *a priori* possibility (11, 13). Wherever it is, plant GGH must be sequestered away from folate polyglutamates, since extractable GGH activities are typically enough to deglutamylate all cellular folate within minutes (7, 10, 11) and treatments that disrupt cellular compartment-

ation cause massive deglutamylation of folates *in situ* (14).

Nor is much known about the subcellular distribution in plants of the folate polyglutamate substrates of GGH, i.e., about the glutamyl tail lengths, one-carbon ($C_1$) substituents, and oxidation state of the folates in different organelles. The only data are for pea leaves, in which penta- and tetraglutamates of 5-formyl-THF and THF appear to predominate in mitochondria, and 5-methyl-THF (of unknown tail length) elsewhere (15-17). There are, however, some data for pea on the distribution of *total* folate. Mitochondria, plastids, and a fraction comprised mainly of the cytosol and vacuole accounted for 11-30%, 3-11%, and 60-80%, respectively, of leaf folate (17-19). Besides not distinguishing among folate forms, these data leave open the key question of whether vacuoles contain folates.

Knowing whether folates or GGH occur in vacuoles is important for several reasons. If vacuoles store folates, the transport or storage processes might be engineered to enhance folate accumulation (20-22). However, if GGH is vacuolar, the situation could be as in mammals, where lysosomes do not store folates but import folate polyglutamates, hydrolyze them, and export monoglutamates (23, 24). GGH also hydrolyzes the *p*-aminobenzoate (*p*ABA) polyglutamates formed by oxidative degradation of folates (11, 25), yielding *p*-aminobenzoylglutamate (*p*ABAGlu$_1$). This may be the first step in the salvage of *p*ABA for folate re-synthesis, a potentially crucial but unexplored process (22).

In this study, we used recombinant *Arabidopsis* GGHs to clarify the features of this enzyme in plants, and showed that GGH is confined to vacuoles. We also determined the types and tail lengths of folates in organelles. This analysis revealed high levels of 5-methyl-THF polyglutamates in vacuoles.

## EXPERIMENTAL PROCEDURES

*Chemicals and Reagents*—Folic acid (PteGlu$_1$), other folates, *p*ABA polyglutamates (*p*ABAGlu$_n$), and poly-γ-L-glutamates (γ-Glu$_n$) were from Schircks Laboratories (Jona, Switzerland). 5,10-Methenyl-THF polyglutamates were made from the corresponding 5-formyl compounds (26). [3',5',7,9,-$^3$H]-Folic acid was from Moravek Biochemicals (Brea, CA). Macerozyme R-10 and Cellulase Onozuka R-10 were from Yakult Honsha (Tokyo, Japan). $Ni^{2+}$-nitriloacetic acid superflow resin was from Qiagen. Percoll was from Amersham Biosciences. Other biochemicals were from Sigma.

*Plant Material*—Pea plants (*Pisum sativum* cv. Laxton's Progress 9) were grown in vermiculite at 16-18°C in 12-h days (75 μE $m^{-2}$ $s^{-1}$, Cool Light fluorescent tubes) for 12-18 days. Water was added only at sowing. Fresh red beet (*Beta vulgaris*) roots were purchased locally and used within 2 days.

*Subcellular Fractionation of Pea Leaves*—Mitochondria and chloroplasts were purified on Percoll gradients (27, 28). Protoplasts, vacuoles, and a cytosol-enriched fraction were prepared by modifying published methods (29, 30). Briefly, expanded leaves were harvested after 12-24 h in the dark or dim light, cut into 1-mm strips, and washed in 10 mM MES/NaOH, pH 5.5, 0.5 M sorbitol, 5 mM $CaCl_2$, 0.05% (w/v) PVP-40. A previously clarified (20,000 × *g*, 20 min) digestion medium containing 20 mg $ml^{-1}$ cellulase and 5 mg $ml^{-1}$ macerozyme in the same buffer was then added (10 ml per g of tissue) followed by incubation at 25°C for 4 h in white fluorescent light (150 μE $m^{-2}$ $s^{-1}$) with rotary shaking (60 rpm). The released protoplasts were filtered through a 70-μm nylon mesh and purified on a three-step sucrose-sorbitol gradient as described (29) except that the buffer contained 5 mM $CaCl_2$ and the density of the bottom layer was increased by adding 10% (v/v) Percoll. A cytosolic fraction was prepared as described (29) from protoplasts washed in 10 mM MOPS-NaOH, pH 7.0, 0.5 M sorbitol, 5 mM $CaCl_2$. To obtain vacuoles, washed protoplast suspensions (3-4 mg chlorophyll $ml^{-1}$ corresponding to 4-5 × $10^7$ protoplasts $ml^{-1}$) were: (i) rapidly diluted 1:10 in 100 mM K-phosphate, pH 8.0, 1 mM dithiothreitol, 1 mM $MgCl_2$, 0.05% (w/v) PVP-40; (ii) gently stirred for 4 min; and (iii) loaded in 1.5-ml aliquots onto a three-step gradient consisting of 5% Ficoll (5 ml, bottom), 3% Ficoll (2 ml, middle), and 0.5% Ficoll (1.5 ml, top), each in the above buffer. This procedure was scaled up as necessary. After centrifugation (30 min, 1,000 × *g*, swinging bucket rotor without braking), intact vacuoles were recovered at the 3%-0.5% Ficoll interface and used without further treatment.

Organelle preparations for folate analysis were supplemented with 10 mM β-mercaptoethanol, frozen in liquid $N_2$, and stored at −80°C. Enzymes were extracted from organelles by freezing in liquid $N_2$ and thawing at 30°C (3-5 cycles), then centrifuging at 16,000 × *g* for 10 min at 4°C. These extracts, and cytosol fractions, were desalted on PD-10 columns (Amersham Biosciences) equilibrated in 100 mM K-phosphate, pH 6.0, 10% glycerol, 10 mM β-mercaptoethanol, 10 mM ascorbic acid, and stored at −80°C after freezing in liquid $N_2$. GGH was assayed as outlined below, and the marker enzymes α-mannosidase, NADP-linked glyceraldehyde-3-phosphate dehydrogenase (GAPDH), fumarase, and methylene tetrahydrofolate reductase (MTHFR) essentially as described (30-32). Fumarase was assayed in a separate set of freshly-prepared extracts not desalted or desalted in 50 mM Tricine-NaOH, pH 8.4.

*Red Beet Root Vacuoles*—Intact vacuoles were isolated essentially as described (33) except that dithiothreitol replaced β-mercaptoethanol and Histodenz™ replaced Metrizamide. Sigma plant protease inhibitor cocktail was added to all media except when vacuoles were assayed for GGH activity. Routinely, 450 g of roots were peeled, cut into 5-mm slices, and loaded into the slicing apparatus, which was set to a slice thickness of 0.1 mm and operated at ~150 rpm. The slices and released cell contents were collected in 1 l of ice-cold 50 mM Tris-HCl, pH 8.0, containing 1 M sorbitol, 5 mM EDTA, 15 mM dithiothreitol, plus or minus 1 ml/l protease inhibitor cocktail, and filtered through two layers of cheesecloth. The solid residue was sliced and filtered again, and the pooled filtrates were centrifuged at 2,000 × *g* for 20 min at 4°C. The vacuole-enriched pellets were resuspended in 20 ml 15% (w/v) Histodenz™ dissolved in buffer A (1.2 M sorbitol, 1 mM EDTA, 15 mM dithiothreitol, 25 mM Tris-MES, pH 8.0, plus or minus 1 ml/l protease inhibitor cocktail). To prepare density gradients, 5-ml aliquots of the suspension in 15-ml disposable clinical centrifuge tubes were successively overlayed with 5 ml 10% (w/v) Histodenz™ in buffer A and 2 ml of buffer A. Gradients were centrifuged at 650 × *g* for 10 min at 4°C and vacuoles were collected from the 0/10% Histodenz™ interface. To remove most of the Histodenz™, the suspension was added to at least 2 volumes of buffer A and centrifuged at 650 × *g* for 5 min at 4°C. The final vacuole pellet was resuspended in 200-500 µl resuspension medium or 200 µl GGH assay buffer (see below), frozen in liquid $N_2$, and held at −80°C until analysis. Betanin contents of vacuoles and samples of the roots they came from were estimated spectrophotometrically ($\varepsilon_{550nm}$ = 62,000 $M^{-1}$ $cm^{-1}$) (34). Betanin was extracted from freeze-dried root samples by grinding in 1 mM EDTA, 50 mM Tris-HCl, pH 7.5, and centrifuging to clarify.

*Folate Analysis*—Folates were extracted and analyzed by HPLC with electrochemical detection as described (21, 35, 36) with the following modifications. Subcellular fraction samples were routinely thawed, made to 10 ml with extraction buffer (50 mM Hepes-50 mM CHES, pH 7.9, 2% (w/v) sodium ascorbate, 10 mM β-mercaptoethanol), split in two, and processed plus or minus treatment with rat plasma conjugase. The folate-binding column was scaled down from 5 to 1 ml, and the volumes of wash and eluting buffers were reduced proportionately. Beet root samples (8 g) were homogenized in 60 ml of extraction buffer; half the extract was conjugase-treated and half not. The HPLC column and mobile phase buffers were as described (21) with a 55-min (for monoglutamates) or 70-min (for polyglutamates) non-linear elution program. Detector response was calibrated using THF, 5-methyl-THF, 5,10-methenyl-THF, 5-formyl-THF, and $PteGlu_1$ standards. Tri- and pentaglutamate forms of 5-methyl-, 5-formyl-, and 5,10-methenyl-THF were used to identify retention times of polyglutamates.

*cDNAs and Expression in Escherichia coli*—ESTs for genes At1g78660 (GenBank™ CF653065) and At1g78680 (GenBank™ AY096428) were obtained from the Deutsches Ressourcenzentrum für Genomforschung (Berlin, Germany) and the *Arabidopsis* Biological Resource Center (Columbus, OH), respectively. Based on sequence alignments, constructs lacking ~20 or ~45 N-terminal residues were designed for each protein (see Supplemental Fig. 1). The corresponding cDNAs were amplified using Pfu polymerase and the primers shown in Table I, digested, and cloned between the NdeI and XhoI sites of pET28b (Novagen, Madison, WI). This fused the hexahistidine tag-containing sequence MGSSHHHHHHSSGLVPRGSHM to the N-terminus of the proteins. Constructs were made in *E. coli* DH10B cells, sequence-verified, and introduced into *E. coli* BL21-CodonPlus®

(DE3)-RIL cells (Stratagene), which were grown at 27°C in LB medium containing 50 μg $ml^{-1}$ kanamycin and 20 μg $ml^{-1}$ chloramphenicol until $A_{600}$ reached 0.6. Isopropyl-D-thiogalactopyranoside was then added (final concentration 1 mM) and incubation was continued for 3 h at 27°C.

*Protein Purification*—Operations were at 0–4°C. Cells from a 50-ml culture were harvested by centrifugation, resuspended in 1 ml of 50 mM K-phosphate, pH 8.0, 1.5 M NaCl, 10 mM β-mercaptoethanol, and broken in a Mini-BeadBeater (Biospec, Bartlesville, OK) using 0.1-mm zirconia/silica beads. After centrifugation (16,000 × *g*, 15 min), the supernatant was subjected to $Ni^{2+}$ chelate affinity chromatography (0.5-ml column) following the manufacturer's protocol. Bound proteins were eluted using 250 mM imidazole and desalted on PD-10 columns in 100 mM K-phosphate, pH 6.0, 10% glycerol, 10 mM β-mercaptoethanol. After storage at 4°C or at −80°C after freezing in liquid $N_2$, the purified enzymes maintained full activity for several weeks and months, respectively. Protein was estimated by Bradford's method (37) using bovine serum albumin as standard.

*Analytical Ultracentrifugation*—Experiments were run using a Beckman XL-I analytical ultracentrifuge and an AN-60-Ti rotor at 25°C. The proteins were dialyzed into 10 mM Na-acetate, pH 5.5, 1 M NaCl, 1 mM dithiothreitol, 1 mM octyl β-glucoside. Buffer viscosity and density and protein partial specific volume ($\bar{\nu}$) were obtained from SEDNTERP software (http://www.jphilo.mailway.com). The $\bar{\nu}$ values for AtGGH1 and AtGGH2 were respectively calculated from amino acid content to be 0.7324 and 0.7351 ml/g at 20°C. In sedimentation velocity studies, sample volume was 0.42 ml, and the reference volume of dialysis buffer was 0.44 ml. The samples were run at 50,000 rpm. Absorption measurements were made at 280 nm for AtGGH1 (0.8 mg/ml) and 230 nm for AtGGH2 (0.1 mg/ml). A single sample was run in each experiment with zero time between scans, $R_{min}$ was set at 6.0, and the samples were scanned from the earliest time until the boundaries reached the cell bottom. The samples were at thermal equilibrium before starting to spin the rotor, which was accelerated directly to 50,000 rpm. The data were analyzed using the c(s) and c(M) methods found in Sedfit (38) (http://www.analyticalultracentrifugation.com). The sedimentation coefficients calculated from the Sedfit program were converted to $S_{20,w}$ values using Sedfit.

*GGH Assay*—Standard assay mixtures contained folate pentaglutamate ($PteGlu_5$) or *p*$ABAGlu_5$ (0.2 mM unless otherwise indicated), 100 mM K-phosphate, pH 6.0, 10% (v/v) glycerol, 10 mM β-mercaptoethanol, and enzyme in a final volume of 100 μl. After incubation for 0-6 h, the reaction was stopped by boiling for 3 min, then centrifuged at 16,000 × *g* for 10 min. Incubation was at 37°C; no substantial difference in reaction rate was observed in the range 30–42°C. Folate- or *p*ABA-containing analytes in the supernatant were separated by HPLC using a C18 Symmetry column (Waters, 7.5 × 0.46 cm; 3 μm particle size) and quantified by absorption at 282 nm (292 nm for 5-methyl-THF) or by fluorescence (270 nm excitation, 350 nm emission), respectively. The column was eluted at 1.5 ml $min^{-1}$ with a 10-min linear gradient from 15% to 45% (v/v) methanol in 50 mM Na-phosphate buffer, pH 6.0, containing 8 mM tetrabutylammonium bisulfate (buffer B). γ-$Glu_n$ and glutamate were derivatized with *o*-phthalaldehyde (39), separated using the column above connected in series to a C18 Spherisorb ODS2 column (Waters, 15 × 0.46 cm; 5 μm particle size) and isocratic elution with 40% methanol buffer B, and quantified fluorometrically (365 nm excitation, 420 nm emission). For kinetic studies, initial rates of substrate disappearance were measured (before an average of 25% of $PteGlu_5$ or 3% of *p*$ABAGlu_5$ had been used). Rates were proportional to enzyme concentration and time. Kinetic constants were calculated from Hanes-Woolf plots. To determine specificity for the various γ-glutamyl bonds in $PteGlu_5$ or *p*$ABAGlu_5$, residual substrate and the various $PteGlu_n$ or *p*$ABAGlu_n$ products were determined, and the extent of hydrolysis (*E*) was plotted *versus* the relative concentration (*R*) of each $PteGlu_n$ or *p*$ABAGlu_n$ species (40). These terms are defined as follows:

$$E = \frac{(XGlu_4 + XGlu_3 + XGlu_2 + XGlu_1)}{(XGlu_5 + XGlu_4 + XGlu_3 + XGlu_2 + XGlu_1)}$$

$$R = \frac{(XGlu_n)}{(XGlu_5 + XGlu_4 + XGlu_3 + XGlu_2 + XGlu_1)}$$

where *X*$Glu_n$ = $PteGlu_n$ or *p*$ABAGlu_n$. The slope of the line corresponding to each product measures

the relative extent of its formation, and so indicates the γ-glutamyl bond specificity of the enzyme.

## RESULTS

*GGH-like Genes in Arabidopsis and Other Plants*—BLAST searches of genome and EST databases at GenBank™ and TIGR indicated that higher plants have one or a few genes encoding proteins similar to mammalian GGHs. For instance, rice and maize appear to have one gene, soybean and cotton two, *Arabidopsis* three, and tomato four. *Arabidopsis* is thus typical in having a small GGH gene family.

The three *Arabidopsis* genes are tandemly arranged on chromosome 1, and specify proteins (AtGGH1, 2, and 3) that are ~35% identical to human GGH and 70-80% identical to each other. As shown in Supplemental Fig. 1, the *Arabidopsis* proteins share many features with mammalian GGHs, including a predicted secretory pathway signal peptide (41, 42), at least one *N*-glycosylation motif (13), and the conserved cysteine and histidine residues that are catalytically essential in human GGH as well as six other conserved residues that may contribute to catalysis or substrate binding (43, 44). In contrast to these similarities, the AtGGH3 sequence has two short insertions near the N-terminus that have no clear-cut counterparts in mammalian GGHs and are absent from all other available plant GGH sequences. Since AtGGH3 appears to be unique to Arabidopsis and thus not of general interest it was not further studied. This enzyme is also far less strongly expressed than AtGGH1 or 2 (Orsomando and Hanson, unpublished).

*Kinetic Characterization of GGH Proteins*—Recombinant AtGGH1 and AtGGH2 were expressed in *E. coli*, removing the signal peptide region and replacing it with a sequence containing a histidine tag as was done for human GGH (43). This strategy gave high levels of both proteins, which were purified by $Ni^{2+}$ affinity chromatography to >90% homogeneity as judged by SDS-PAGE (see Supplemental Fig. 2). Two versions of each enzyme were made, differing in how many residues were removed (see Supplemental Fig. 1). As results for both versions were similar we report data only for the shorter one. Enzyme assays were made at pH 6.0, which was shown to be near the optimum for both enzymes (6.5-7.0 for AtGGH1 and 6.5 for AtGGH2) and is also close to the pH of the vacuole (in which GGHs are located, see below).

The mode of action and specificity of purified AtGGH1 and AtGGH2 were studied using the pentaglutamates of folic acid ($PteGlu_5$) and *p*ABA (*p*ABA$Glu_5$) as substrates (Fig. 1, *B* and *C*). In the initial stage of $PteGlu_5$ hydrolysis, AtGGH1 formed $PteGlu_2$ and $PteGlu_3$ at similar rates, whereas AtGGH2 formed $PteGlu_1$ and a small amount of $PteGlu_2$ (Fig. 1*B*). This indicates that both enzymes have an endopeptidase action, with AtGGH1 showing an almost equal preference for the second and third γ-glutamyl bonds (counting from the folate moiety) and AtGGH2 preferring the first. This difference in specificity was also evident when *p*ABA$Glu_5$ was the substrate, with an additional cleavage at lower frequency of the fourth γ-glutamyl bond catalyzed by AtGGH2 (Fig. 1*C*).

The kinetic constants for AtGGH1 and AtGGH2 with $PteGlu_5$ or *p*ABA$Glu_5$ as substrate are shown in Table II. The $K_m$ values for $PteGlu_5$ for both enzymes were lower than those reported for a purified pea GGH preparation, and similar to those found for mammalian GGHs, which are typically < 2 μM. As judged from the $K_{cat}/K_m$ ratios, both enzymes hydrolyzed *p*ABA$Glu_5$ less efficiently than $PteGlu_5$.

Further distinctions between the two enzymes appeared when long incubation periods were used to define the end-products of the reaction (Fig. 2). When AtGGH1 acted on $PteGlu_5$, the $PteGlu_3$ formed initially – but not the $PteGlu_2$ – was further hydrolyzed to $PteGlu_1$, so that the final folate products included $PteGlu_1$ as well as $PteGlu_2$ and $PteGlu_3$ (Fig. 2*A*). The other products were γ-$Glu_3$ and γ-$Glu_2$, which were not attacked (Fig. 2*B*). In contrast, AtGGH2 gave only $PteGlu_1$ as the final folate product, although some $PteGlu_2$ accumulated transiently (Fig. 2*A*). The other products of AtGGH2 cleavage were γ-$Glu_5$, γ-$Glu_4$, γ-$Glu_3$, γ-$Glu_2$ and glutamate, with γ-$Glu_5$ and γ-$Glu_4$ disappearing as the reaction progressed (Fig. 2*B*). The unexpected formation of γ-$Glu_5$ is considered below. The results with *p*ABA$Glu_5$ as substrate resembled those with $PteGlu_5$ except that AtGGH1 did not further hydrolyze *p*ABA$Glu_3$, and AtGGH2 produced a small, transient peak of *p*ABA$Glu_4$ and did not further hydrolyze *p*ABA$Glu_2$ (Fig. 2, *C* and *D*). The kinetics of appearance of glutamate and γ-$Glu_n$ (Fig. 2, *B* and *D*) indicated that AtGGH1 does not attack γ-glutamyl pept-

ides released from $PteGlu_5$ or $pABAGlu_5$, while AtGGH2 does so *via* exopeptidase action, the early accumulation of $\gamma$-$Glu_4$ being followed by $\gamma$-$Glu_3$ and later by $\gamma$-$Glu_2$ and $\gamma$-$Glu_1$. This was confirmed by using $\gamma$-$Glu_5$ as substrate (not shown).

Formation of $\gamma$-$Glu_5$ by AtGGH2 (Fig. 2, *B* and *D*) was not due to cleavage of the bond between glutamate and *p*ABA because there was no decline in total $PteGlu_n$ or $pABAGlu_n$ during the reaction (Fig. 2, *A* and *C*) and no pteroic acid was released from $PteGlu_5$, or *p*ABA from $pABAGlu_5$. This was confirmed by demonstrating that, like mammalian GGHs (13), neither plant enzyme attacks $PteGlu_1$ or $pABAGlu_1$ (not shown). The $\gamma$-$Glu_5$ thus presumably came from transpeptidation between the $\gamma$-$Glu_n$ products released from Pte- or $pABAGlu_5$. Transpeptidase activity is common among peptidases, although not previously reported for GGH. Transpeptidation can also explain why no glutamate counterpart to the $pABAGlu_4$ formed was seen for AtGGH2 acting on $pABAGlu_5$ (Fig. 2, *C* and *D*).

*Native Molecular Mass*—Purified recombinant enzymes were analyzed by analytical ultracentrifugation in sedimentation velocity experiments. Each protein yielded a single component in the analysis. For AtGGH1 the $S_{20,w}$ value from the c(s) method was 4.57 S corresponding to a molecular mass of 69.8 kDa calculated using the c(M) method. For AtGGH2 the $S_{20,w}$ was 4.43 S and the calculated mass was 66.0 kDa. These values are close to twice the calculated masses of the recombinant AtGGH1 and AtGGH2 polypeptides (36.7 and 36.4 kDa, respectively), indicating that both enzymes exist as dimers, as does human GGH (44). In this connection, it is noteworthy that the dimer interface regions of the human enzyme (44) are substantially conserved in the plant sequences (see Supplemental Fig. 1).

*Subcellular Localization of GGH Activity*—GGH was localized by cell fractionation and enzyme assay. Pea leaves were used because they are the tissue of choice for obtaining high yields of intact vacuoles and other organelles (27-29) and have been the object of much prior work in folate biochemistry (11, 15-19). The distribution of marker enzyme activities confirmed that purified chloroplasts, mitochondria, and vacuoles were essentially uncontaminated by other fractions (Fig. 3). The vacuole fraction contained $\leq$ 1-2% of the total activities of the cytosol marker MTHFR and the peroxisomal marker catalase (not shown). (Such slight contamination of vacuole preparations is too small to complicate interpretation of the vacuolar folate data to be presented below.) The distribution of GGH activity closely paralleled that of the vacuolar marker $\alpha$-mannosidase (Fig. 3), indicating that GGH is an exclusively vacuolar enzyme. To corroborate this result, we analyzed vacuoles from red beet roots, a classical plant vacuole system. The ratios between GGH activity and the solely vacuolar pigment betanin (34) in vacuoles and whole roots were, respectively, 29.8 ± 3.5 and 21.0 ± 3.3 pmol $min^{-1}$ $\mu mol^{-1}$ (mean ± S.E.), indicating that GGH activity is entirely vacuolar. GGH activities in beet vacuoles were far lower than those in pea vacuoles (11 ± 1 *versus* 2,320 ± 420 pmol $min^{-1}$ $mg^{-1}$ protein, respectively).

*Subcellular Localization of Pea Leaf Folates*—Purified organelle preparations and mesophyll protoplasts were first analyzed after removing polyglutamyl tails to enable identification and quantification of the types of folate (i.e., THF and its $C_1$-substituted forms). The protoplast values (Fig. 4, *top frame*) agree with published total folate contents of pea leaves (16-19), and show a typical distribution of folate types for leaves of pea and other plants (5, 16). (The acidic HPLC mobile phase used in the analysis converts 10-formyl-THF to 5,10-methenyl-THF, so that the 5,10-methenyl-THF measurements include 10-formyl-THF plus any preexisting 5,10-methenyl-THF.) The total folate levels found in mitochondria and chloroplasts (about 50% and 10%, respectively, of cellular folates) also agree with literature values (16-19), as does the finding that 5-formyl-THF is the major folate in mitochondria (16, 17). The most striking result is that vacuoles contain a substantial amount of folate, almost all as 5-methyl-THF (Fig. 4, *bottom frame*). That this is not contamination by other fractions is attested by the enzyme marker data (see above) and by the distribution of folate types, which differs from those of other fractions (Fig. 4). The absence of significant contamination was further confirmed by adding tracer [$^3$H]folic acid to the protoplast lysates from which vacuoles were isolated; the purified vacuoles accounted for $\leq$0.5% of the $^3$H added (data not shown).

To estimate the percentage of total cellular folate and 5-methyl-THF present in vacuoles, the folate contents of vacuole preparations and the

protoplasts from which they came were expressed relative to the activity of α-mannosidase, which is specific to vacuoles in plants (45). Among three separate preparations, an average of 20% of total folate was vacuolar, and 38% of the 5-methyl-THF (Table III).

*Polyglutamylation of Pea Leaf Organellar Folates*—The extent of polyglutamylation was determined for the major folate in each organelle (Fig. 5). The main mitochondrial folate, 5-formyl-THF, existed mainly as penta- and hexaglutamates (similar to a previous report, Ref. 15) as did 5,10-methenyl-THF in chloroplasts. Half the vacuolar 5-methyl-THF was also polyglutamylated although the average tail length was shorter than in the other organelles. The survival of *any* polyglutamyl folate in the vacuole was unexpected as GGH activity is in theory high enough to deglutamylate most of the vacuolar folate in less than a minute (see "*Discussion*" for the calculation).

To confirm that the persistence of vacuolar 5-methyl-THF polyglutamates is not simply because plant GGHs do not attack them, we compared 5-methyl-THF pentaglutamate and $PteGlu_5$ as substrates for purified AtGGH1 and 2, and for the GGH activity in pea vacuole extracts. At the physiological concentration of 1 μM, both substrates were hydrolyzed at similar rates by all three enzyme preparations. The observed activities (nmol $min^{-1}$ $mg^{-1}$ protein, with 5-methyl-THF pentaglutamate and $PteGlu_5$, respectively) were: AtGGH1 3,690 and 5,200; AtGGH2 3,590 and 4,120; pea GGH 1.9 and 2.8.

*Analysis of Beet Root Folates*—To explore the generality of the findings above, we analyzed red beet roots and their vacuoles. The principal folate in root tissue was 5-methyl-THF, in accord with published data for beets and other storage organs (46) (Fig. 6*A*). As with pea vacuoles, beet vacuoles contained substantial levels of 5-methyl-THF (Fig. 6*A*). The amounts of 5-methyl-THF in beet vacuoles were quantified by relating the folate contents of vacuole preparations and root tissue to their betanin contents (Table IV). In five independent preparations, from 16 to 60% of the 5-methyl-THF was vacuolar. The vacuolar 5-methyl-THF was 76% polyglutamylated, with di- and pentaglutamates predominant (Fig. 6*B*). Since beet vacuoles also contain GGH, the situation in beet is like that in pea: folyl polyglutamates and the enzyme that hydrolyzes them co-exist in vacuoles.

## DISCUSSION

Our results establish that plant GGHs are broadly similar in structure and catalytic properties to those of mammals, as suggested by other reports (8-11). Like mammalian GGHs (13, 47), the *Arabidopsis* enzymes studied are dimers of ~300-residue polypeptides, have mildly acidic pH optima, attack both *p*ABA and folate polyglutamates, and show different cleavage patterns despite having similar amino acid sequences. AtGGH1 and AtGGH2 both act as endopeptidases but they prefer different bonds and only AtGGH2 attacks $PteGlu_2$. Since $PteGlu_2$ is a major product of AtGGH1 action, the two enzymes, in a sense, complement each other. Such complementarity may have confounded specificity studies of plant GGHs made with crude extracts or mixed isoforms (8, 9). AtGGH2 also shows exopeptidase and transpeptidase action on $\gamma$-$Glu_n$ products.

The *Arabidopsis* GGH proteins and all other plant GGH sequences available have an *N*-glycosylation motif in a conserved position, suggesting that they exist naturally as glycoproteins, as do mammalian GGHs (13). Even though mammalian GGHs have four or more potential *N*-glycosylation sites and are heavily glycosylated, the recombinant proteins produced in *E. coli* have similar biochemical characteristics to their glycosylated counterparts (48-50). It is therefore likely that the *E. coli*-derived *Arabidopsis* GGHs used in our study faithfully mirror the properties of the enzymes as they exist *in planta*.

Our finding that pea GGH activity is vacuolar is supported by the recent detection of AtGGH2 and AtGGH3 proteins in *Arabidopsis* leaf vacuoles (42) and fits with the presence of signal peptides, which occur in many vacuole-associated proteins (42, 51) and participate in vacuolar sorting (52). The vacuolar site parallels the lysosomal location of intracellular mammalian GGH (13, 47), for lysosomes and central vacuoles of plants are both lytic compartments (53). An exclusively vacuolar location seems hard to reconcile with previous reports that GGH is cytosolic or extracellular, but this is not the case. The cytosolic location was inferred by fractionating extracts prepared by chopping, which breaks many vacuoles, and in fact 19% of the GGH activity *was* in the vacuole fraction (11). The apoplastic location was based on there being a GGH-like protein in extracellular wash

fluid of soybean leaves; GGH activity was not assayed (12). Isolation of the corresponding cDNA (8) and cognate ESTs has since shown that this protein, unlike all other plant GGH sequences, lacks two catalytically essential residues (Cys110 and His220 in the human enzyme) (43). It thus appears that soybean cells secrete into the apoplast an unusual GGH-like protein, not an active GGH enzyme.

Our analyses of organellar folates show that each organelle has a distinct folate profile. The mitochondrial profile is dominated by 5-formyl-THF, which is not a $C_1$ donor but an inhibitor of folate-dependent enzymes (54). 5-Formyl-THF is recycled to the active $C_1$ folate pool by a cyclo-ligase that is mitochondrial in plants (55). The chloroplast folate pool is richest in 5,10-methenyl-THF (which is generated during our analysis from 10-formyl-THF) but also contains 5-methyl-THF, whose occurence in chloroplasts has previously been inferred from the presence of the enzyme that uses it, methionine synthase (56). The folate pools of both leaf and storage root vacuoles proved to consist almost entirely of 5-methyl-THF, suggesting a storage role for this folate. 5-Methyl-THF seems a plausible candidate for storage because it is quite stable and is readily converted to other $C_1$ folates *via* the reversible MTHFR reaction in plants (32). Although vacuolar storage pools of folate have not been reported before, their existence might have been predicted from the lack of correlation between folate levels and $C_1$ metabolic activity, and the wide variation in folate levels between comparable tissues from different species (57). Beet roots are a good example – although metabolically quiescent their folate levels are as high as those in green leaves, and far higher than those of other storage roots (57).

The observed polyglutamylation of vacuolar folates is paradoxical because the glutamyl tail is not expected to survive long in the presence of the GGH activity, as the following calculation shows. For pea leaves, assuming that the vacuole is 70% of the water volume (58), and that total folate content is 5 nmol $g^{-1}$ fresh weight (17), the folyl-polyglutamate level (Table III and Fig. 5) would be ~1 nmol $ml^{-1}$. The vacuolar GGH activity (2.3 nmol $min^{-1}$ $mg^{-1}$ protein, see Fig. 3) is equivalent to ~8 nmol $min^{-1}$ $ml^{-1}$ vacuolar contents at $V_{max}$, or ~4 nmol $min^{-1}$ $ml^{-1}$ at a folate concentration of ~1 nmol $ml^{-1}$ (estimated from the vacuolar folate concentration above, the folate and GGH contents expressed per unit protein, and the $K_m$ values for the *Arabidopsis* enzymes). Under steady-state conditions, the vacuolar folyl polyglutamates therefore have a predicted half-life of ~7 sec. A similar calculation for beet root vacuoles indicates a polyglutamate half-life of ~5 min. These calculations assume that pea and beet GGHs behave similarly to a mixture of the *Arabidopsis* enzymes. Partial characterization of the activities in pea and beet vacuole extracts supported this assumption. The calculations also assume that GGH and folyl polyglutamates show no tendency to be segregated into distinct vacuole subpopulations within cells.

Chloroplasts and mitochondria contain isoforms of folylpolyglutamate synthetase (6) as well as the ATP that this enzyme requires. The presence of polyglutamates in these organelles is therefore easily explained by *in-situ* synthesis from monoglutamyl folates. Not so for vacuoles, which most probably contain neither the synthetase (6) nor ATP (59). For vacuoles it is thus necessary to invoke – as for mammalian lysosomes (23, 24) – import of folylpolyglutamates by a carrier-mediated process.

The co-occurrence of folylpolyglutamates and GGH in vacuoles could be explained by the presence of a potent GGH inhibitor, or by folate-binding proteins that protect polyglutamates from hydrolysis. There is so far no experimental evidence for or against either possibility. However, inhibiting GGH action on folylpolyglutamates would also stop *p*ABA polyglutamate hydrolysis and so could disrupt folate recycling. Folate-binding proteins are therefore perhaps a more attractive solution. Various such proteins have been characterized in mammals (60) and shown to protect bound folates against both cleavage of the polyglutamyl tail and oxidative degradation (1, 39).

*Acknowledgements*—We thank Dr. Bala Rathinasabapathi for advice on protoplast isolation, Dr. Eoin Quinlivan for advice on HPLC, Drs. Carole Dabney-Smith and Fabien Gerard for chloroplast preparations, and Ms. Leslie Eisele of the Wadsworth Center Biochemistry Shared Instrumentation Core Facility for performing the analytical ultracentrifugation experiments.

## REFERENCES


1. Scott, J., Rébeillé, F., and Fletcher, J. (2000) *J. Sci. Food Agric.* **80,** 795-824
2. Zheng, L.-L., Lin, Y., Lin, S., and Cossins, E. A. (1992) *Phytochemistry* **31,** 2277-2282
3. Shane, B. (1989) *Vitam. Horm.* **45,** 263-335
4. Brzezińska, A., Wińska, P., and Balińska, M. (2000) *Acta Biochim. Pol.* **47,** 735-749
5. Cossins, E. A. (2000) *Can. J. Bot.* **78,** 691-708
6. Ravanel, S., Cherest, H., Jabrin, S., Grunwald, D., Surdin-Kerjan, Y., Douce, R., and Rébeillé, F. (2001) *Proc. Natl. Acad. Sci. USA* **98,** 15360-15365
7. Leichter, J., Landymore, A. F., and Krumdieck, C. L. (1979) *Am. J. Clin. Nutr.* **32,** 92-95
8. Huangpu, J., Pak, J. H., Burkhart, W., Graham, M. C., Rickle, S., Liu, C. Y., and Graham, J. S. (1996) *Plant Physiol.* **112,** 862
9. Rickle, S. A., Xu, H., Liu, C. Y., Morris, P. F., and Graham, J. S. (1998) *Plant Physiol.* **117,** 1526
10. Wu, K., Cossins, E. A., and King, J. (1994) *Plant Physiol.* **104,** 373-380
11. Lin, S., Rogiers, S., and Cossins, E. A. (1993) *Phytochemistry* **32,** 1109-1117
12. Huangpu, J., Pak, J. H., Graham, M. C., Rickle, S. A., and Graham, J. S. (1996) *Biochem. Biophys. Res. Commun.* **228,** 1-6
13. Galivan, J., Ryan, T. J., Chave, K., Rhee, M., Yao, R., and Yin, D. (2000) *Pharmacol. Ther.* **85,** 207-215
14. Melse-Boonstra, A., Verhoef, P., Konings, E. J., Van Dusseldorp, M., Matser, A., Hollman, P. C., Meyboom, S., Kok, F. J., and West, C. E. (2002) *J. Agric. Food Chem.* **50,** 3473-3478
15. Besson, V., Rébeillé, F., Neuburger, M., Douce, R., and Cossins, E. A. (1993) *Biochem. J.* **292,** 425-430
16. Chen, L., Chan, S.Y., and Cossins, E. A. (1997) *Plant Physiol.* **115,** 299-309
17. Chan, S. Y., and Cossins, E. A. (2003) *Pteridines* **14,** 67-76
18. Gambonnet, B., Jabrin, S., Ravanel, S., Karan, M., Douce, R., and Rébeillé, F. (2001) *J. Sci. Food Agric.* **81,** 835-841
19. Jabrin, S., Ravanel, S., Gambonnet, B., Douce, R., and Rébeillé, F. (2003) *Plant Physiol.* **131,** 1431-1439
20. Hossain, T., Rosenberg, I., Selhub, J., Kishore, G., Beachy, R., and Schubert, K. (2004) *Proc. Natl. Acad. Sci. USA* **101,** 5158-5163
21. Diaz de la Garza, R., Quinlivan, E. P., Klaus, S. M., Basset, G. J., Gregory, J. F. 3rd, and Hanson, A. D. (2004) *Proc. Natl. Acad. Sci. USA* **101,** 13720-13725
22. Hanson, A. D., and Gregory, J. F. 3rd (2002) *Curr. Opin. Plant Biol.* **5,** 244-249
23. Sirotnak, F. M., and Tolner, B. (1999) *Annu. Rev. Nutr.* **19,** 91-122
24. Barrueco, J. R., O'Leary, D. F., and Sirotnak, F. M. (1992) *J. Biol. Chem.* **267,** 15356-15361
25. Suh, J. R., Herbig, A. K., and Stover, P. J. (2001) *Annu. Rev. Nutr.* **21,** 255-282
26. Schirch, V. (1997) *Methods Enzymol.* **281,** 81-87
27. Douce, R., Bourguignon, J., Brouquisse, R., and Neuburger, M. (1987) *Methods Enzymol.* **148,** 403-415
28. Cline, K. (1986) *J. Biol. Chem.* **261,** 14804-14810
29. Baldet, P., Alban, C., Axiotis, S., and Douce, R. (1993) *Arch. Biochem. Biophys.* **303,** 67-73
30. Trossat, C., Nolte, K. D., and Hanson, A. D. (1996) *Plant Physiol.* **111,** 965-973
31. Nok, A. J., Shuaibu, M. N., Kanbara, H., and Yanagi, T. (2000) *Parasitol. Res.* **86,** 923-928
32. Roje, S., Wang, H., McNeil, S. D., Raymond, R. K., Appling, D. R., Shachar-Hill, Y., Bohnert, H. J., and Hanson, A. D. (1999) *J. Biol. Chem.* **274,** 36089-36096
33. Leigh, R. A., and Branton, D. (1976) *Plant Physiol.* **58,** 656-662
34. Leigh, R. A., ap Rees, T., Fuller, W. A., and Banfield, J. (1979) *Biochem. J.* **178,** 539-547
35. Gregory, J. F. 3rd, and Toth, J. P. (1988) *Anal. Biochem.* **170,** 94-104
36. Bagley, P. J., and Selhub, J. (2000) *Clin. Chem.* **46,** 404-411
37. Bradford, M. M. (1976) *Anal. Biochem.* **72,** 248-254

38. Schuck, P. (2000) *Biophys. J.* **78,** 1606-1619
39. Wang, Y., Nimec, Z., Ryan, T. J., Dias, J. A., and Galivan, J. (1993) *Biochim. Biophys. Acta* **1164,** 227-235
40. Bhandari, S. D., Gregory, J. F. 3rd, Renuart, D. R., and Merritt, A. M. (1990) *J. Nutr.* **120,** 467-475
41. Bendtsen, J. D., Nielsen, H., von Heijne, G., and Brunak, S. (2004) *J. Mol. Biol.* **340,** 783-795
42. Carter, C., Pan, S., Zouhar, J., Avila, E. L., Girke, T., and Raikhel, N. V. (2004) *Plant Cell* **16,** 3285-3303
43. Chave, K. J., Auger, I. E., Galivan, J., and Ryan, T. J. (2000) *J. Biol. Chem.* **275,** 40365-40370
44. Li, H., Ryan, T. J., Chave, K. J., and Van Roey, P. (2002) *J. Biol. Chem.* **277,** 24522-24529
45. Ahmed, S. U., Rojo, E., Kovaleva, V., Venkataraman, S., Dombrowski, J. E., Matsuoka, K., and Raikhel, N. V. (2000) *J. Cell Biol.* **149,** 1335-1344
46. Konings, E. J., Roomans, H. H., Dorant, E., Goldbohm, R. A., Saris, W. H., and van den Brandt, P. A. (2001) *Am. J. Clin. Nutr.* **73,** 765-776
47. McGuire, J. J., and Coward, J. K. (1984) in *Folates and Pterins,* Vol. 1 (Blakley, R. L., and Benkovic, S. J., eds) pp. 135-190, Wiley, New York
48. Yao, R., Nimec, Z., Ryan, T. J., and Galivan, J. (1996) *J. Biol. Chem.* **271,** 8525-8528
49. Yao, R., Schneider, E., Ryan, T. J., and Galivan, J. (1996) *Proc. Natl. Acad. Sci. USA* **93,** 10134-10138
50. Rhee, M. S., Lindau-Shepard, B., Chave, K. J., Galivan, J., and Ryan, T. J. (1998) *Mol. Pharmacol.* **53,** 1040-1046
51. Shimaoka, T., Ohnishi, M., Sazuka, T., Mitsuhashi, N., Hara-Nishimura, I., Shimazaki, K., Maeshima, M., Yokota, A., Tomizawa, K., and Mimura, T. (2004) *Plant Cell Physiol.* **45,** 672-683
52. Vitale, A., and Chrispeels, M. J. (1992) *Bioessays* **14,** 151-160
53. Kuriyama, H., and Fukuda, H. (2002) *Curr. Opin. Plant Biol.* **5,** 568-573
54. Stover, P., and Schirch, V. (1993) *Trends Biochem. Sci.* **18,** 102-106
55. Roje, S., Janave, M. T., Ziemak, M. J., and Hanson, A. D. (2002) *J. Biol. Chem.* **277,** 42748-42754
56. Ravanel, S., Block, M. A., Rippert, P., Jabrin, S., Curien, G., Rébeillé, F., and Douce, R. (2004) *J. Biol. Chem.* **279,** 22548-22557
57. Royal Society of Chemistry/MAFF (1991) *McCance and Widdowson's 'The Compostion of Foods'* 5th Ed. and Supplements, Royal Society of Chemistry/Ministry of Agriculture, Fisheries, and Food, Cambridge
58. Winter, H., Robinson, D. G., and Heldt, H. W. (1994) *Planta* **193,** 530-535
59. Farré, E. M., Tiessen, A., Roessner, U., Geigenberger, P., Trethewey, R. N., and Willmitzer, L. (2001) *Plant Physiol.* **127,** 685-700
60. Henderson, G. B. (1990) *Annu. Rev. Nutr.* **10,** 319-335

## FOOTNOTES

*This work was supported in part by the Florida Agricultural Experimental Station, by an endowment from the C.V. Griffin, Sr. Foundation, by grant no. R01 GM071382-01 from the National Institutes of Health, by grant no. MCB-0443709 from the National Science Foundation, and approved for publication as Journal Series no. R-10872.

**To whom correspondence should be addressed: Horticultural Sciences Department, University of Florida, P.O. Box 110690, Gainesville, Florida 32611. Tel.: 352-392-1928; Fax: 352-392-5653; E-mail: adha@mail.ifas.ufl.edu

[1]The abbreviations used are: *p*ABA, *p*-aminobenzoic acid; *p*ABAGlu$_1$, *p*-aminobenzoylmonoglutamate; *p*ABAGlu$_n$, *p*-aminobenzoylpolyglutamate; $C_1$, one-carbon; GAPDH, NADP-linked glyceraldehyde-3-phosphate dehydrogenase; GGH, γ-glutamyl hydrolase; γ-Glu$_n$, poly-γ-L-glutamate; MTHFR, methylenetetrahydrofolate reductase; PteGlu$_1$, folic acid; PteGlu$_n$, folate polyglutamate; THF, tetrahydrofolate.

## FIGURE LEGENDS

**FIG. 1. Structures of GGH substrates and the bond cleavage specificity of *Arabidopsis* GGHs.** *A*, the structure of folyl and *p*ABA polyglutamates (the folate shown is THF). One-carbon units at various oxidation levels (formyl, methyl, etc.) are attached to $N^5$ and/or $N^{10}$ of the folate moiety. Oxidative degradation of folyl polyglutamates results in cleavage of the $C^9$-$N^{10}$ bond, yielding a pterin and *p*-aminobenzoylglutamate (*p*ABAGlu$_1$) with a polyglutamyl tail. *B* and *C*, progress curves for the initial stages of hydrolysis of PteGlu$_5$ (*B*) and *p*ABAGlu$_5$ (*C*) by purified recombinant AtGGH1 or AtGGH2. The substrate concentration supplied was 0.2 mM. Data are presented as plots of relative concentration of each reaction product *versus* extent of reaction (see *"Experimental Procedures"*) and are pooled values from two representative experiments.

**FIG. 2. Kinetics of product formation during the prolonged action of AtGGH1 or AtGGH2 on pentaglutamate substrates.** Initial substrate concentrations were 0.2 mM. Data are presented in units of nmol/20-µl reaction. *A*, folate-containing products formed from PteGlu$_5$. *B*, glutamate and γ-Glu$_n$ products formed from PteGlu$_5$. *C*, *p*ABA-containing products formed from *p*ABAGlu$_5$. *D*, glutamate and γ-Glu$_n$ products formed from *p*ABAGlu$_5$. Numerals (*1* to *5*) by curves indicate the number of glutamyl residues in each product. Data are from representative individual experiments, which were repeated at least three times with similar results.

**FIG. 3. Localization of GGH in pea leaf vacuoles by subcellular fractionation.** Chloroplasts (*CP*), mitochondria (*M*), and vacuoles (*V*) were purified by density gradient centrifugation. A fraction enriched in cytosol and vacuole contents (*CS+V*) was prepared from pea leaf protoplasts by pelleting intact organelles. The specific activities (units mg$^{-1}$ protein) of GGH (measured using *p*ABAGlu$_5$) and marker enzymes were assayed in each fraction. Markers were: α-mannosidase (vacuole); NADP-linked glyceraldehyde-3-phosphate dehydrogenase (*GAPDH*, chloroplast); fumarase (mitochondrion); and methylenetetrahydrofolate reductase (*MTHFR*, cytosol). The *asterisk* indicates that a trace of MTHFR activity was detectable in vacuoles, but was too low to quantify; it represented ≤ 2% of the total activity of the protoplasts. Data are means and S.E. of data from three to ten independent preparations of each fraction.

**FIG. 4. Types of folates in organelles from pea leaves.** Mitochondria, chloroplasts, and vacuoles were purified by density gradient centrifugation and shown to be free of significant contamination by other fractions, as in Fig. 3. Mesophyll protoplasts were analyzed for comparison. Folates were deglutamylated before HPLC analysis with electrochemical detection. Data are means and S.E. values from three independent organelle or protoplast preparations. In addition to the folates shown, small amounts (~2% of total folate) of folic acid and 10-formyldihydrofolate were found in chloroplasts and mitochondria, respectively. *5-CH$_3$-THF*, 5-methyl-THF; *5-CHO-THF*, 5-formyl-THF; *5,10=CH-THF*, 5,10-methenyl-THF.

**FIG. 5. Distribution of polyglutamyl tail lengths of the main folate types in organelles from pea leaves.** The organelle preparations analyzed were the same as in Fig. 4. HPLC analysis with electrochemical detection was used to analyze the tail length distribution for the predominant type of folate in each organelle, i.e., 5-formyl-THF (*5-CHO-THF*) in mitochondria, 5,10-methenyl-THF (*5,10=CH-THF*) in chloroplasts, and 5-methyl-THF (*5-CH$_3$-THF*) in vacuoles. Data are means and S.D. of data from three independent organelle preparations.

**FIG. 6. Analysis of folate types and polyglutamyl tail lengths in red beet roots and vacuoles.** Vacuoles were purified by density gradient centrifugation. Folate types (*A*) and the tail length of 5-methyl-THF (*B*) were analyzed by HPLC with electrochemical detection. Data are means and S.E. (*A*) or S.D. (*B*) for four independent vacuole preparations and samples of the roots from which each preparation was made. *5-CH$_3$-THF*, 5-methyl-THF; *5-CHO-THF*, 5-formyl-THF; *5,10=CH-THF*, 5,10-methenyl-THF.

## TABLE I

*PCR primers used to clone truncated Arabidopsis GGH sequences into pET28b*

NdeI and XhoI sites are underlined. FL, forward primer for long version; FS, forward primer for short version; R, reverse primer.

| Gene | | Primer sequence (5' → 3') |
|---|---|---|
| AtGGH1 | FL: | GATCGATCCATATGGAGGCTTCTGAGTCGATT |
| (At1g78660) | FS: | GATCGATCCATATGGTTTGCTCCTCGCCGGAT |
| | R: | TGATCCTCGAGTTAGAAACGGGATCTTGGTT |
| AtGGH2 | FL: | GATCGATCCATATGGCCAAGGCTGCGACG |
| (At1g78680) | FS: | GATCGATCCATATGGTATGCTCTGCTCCGGAT |
| | R: | TGATCCTCGAGTTAGAGAAGGGATCGTTGTT |

## TABLE II

*Kinetic constants of AtGGH1 and AtGGH2 with $PteGlu_5$ or $pABAGlu_5$ as substrate*

Values were determined at 37°C in 100 mM K-phosphate buffer, pH 6.0, 10% (v/v) glycerol, 10 mM β-mercaptoethanol, using substrate concentrations of 0.5-10 μM. Data are means of three independent determinations ± S.E.

| Enzyme | $PteGlu_5$ | | | $pABAGlu_5$ | | |
|---|---|---|---|---|---|---|
| | $K_m$ | $K_{cat}$ | $K_{cat}/K_m$ | $K_m$ | $K_{cat}$ | $K_{cat}/K_m$ |
| | $\mu M$ | $s^{-1}$ | $s^{-1}\ M^{-1}$ | $\mu M$ | $s^{-1}$ | $s^{-1}\ M^{-1}$ |
| AtGGH1 | 0.79 ± 0.04 | 19.46 ± 0.52 | $2.46 \times 10^7$ | 1.50 ± 0.22 | 8.29 ± 0.74 | $5.53 \times 10^6$ |
| AtGGH2 | 0.52 ± 0.07 | 8.74 ± 0.49 | $1.68 \times 10^7$ | 1.86 ± 0.20 | 5.51 ± 0.61 | $2.97 \times 10^6$ |

## TABLE III

*Total folate and 5-methyl-THF contents of pea leaf mesophyll protoplasts and vacuoles*

Total folate and 5-methyl-THF were determined in three independent protoplast preparations and in the vacuoles derived from them, and expressed relative to the activities of the vacuolar marker α-mannosidase. One α-mannosidase unit (*U*) = 1 μmol of substrate hydrolyzed $min^{-1}$.

| Preparation | Total folate | | | 5-Methyl-THF | | |
|---|---|---|---|---|---|---|
| | Protoplasts | Vacuoles | Vacuolar folate | Protoplasts | Vacuoles | Vacuolar 5-methyl-THF |
| | *pmol/U* | | *%* | *pmol/U* | | *%* |
| 1 | 19.4 | 2.4 | 12 | 10.6 | 2.4 | 20 |
| 2 | 20.1 | 5.5 | 27 | 9.6 | 5.0 | 52 |
| 3 | 15.6 | 3.6 | 23 | 7.5 | 3.2 | 42 |

## TABLE IV

*5-Methyl-THF contents of red beet root tissue and vacuoles*

5-Methyl-THF was determined in independent root tissue samples and in vacuoles derived from them, and expressed relative to the level of the vacuolar marker betanin.

| Preparation | 5-Methyl-THF | | |
|---|---|---|---|
| | Root tissue | Vacuoles | Vacuolar 5-methyl-THF |
| | *nmol μmol$^{-1}$ betanin* | | *%* |
| 1 | 3.80 | 1.01 | 27 |
| 2 | 4.31 | 1.00 | 23 |
| 3 | 2.16 | 0.68 | 32 |
| 4 | 1.43 | 0.23 | 16 |
| 5[a] | 2.08 | 1.25 | 60 |

[a] Three vacuole preparations were pooled for this analysis.

# Supplemental Figure 1

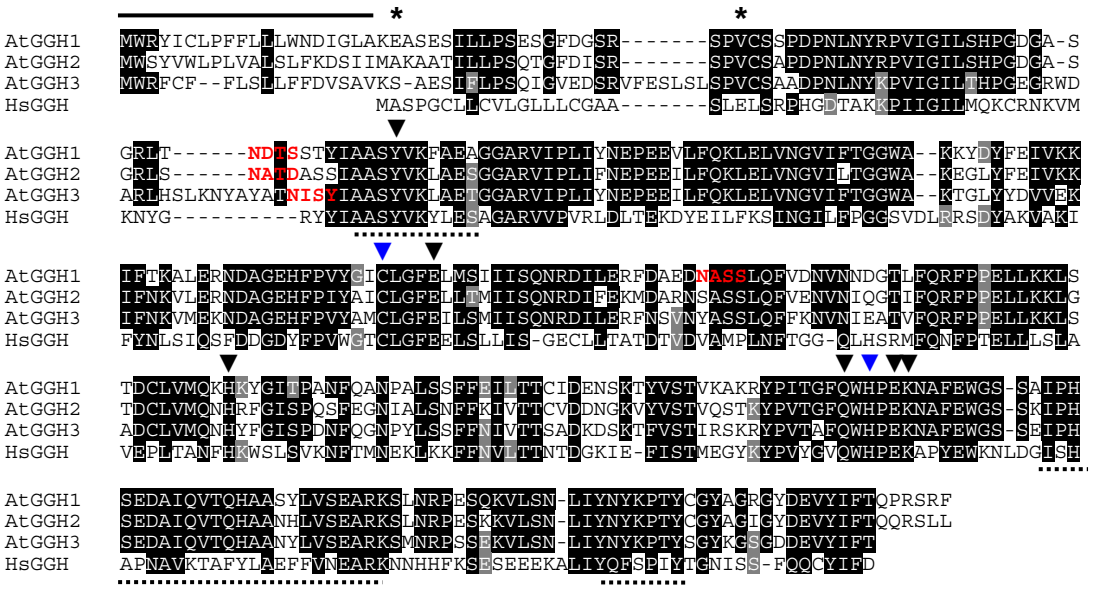


Alignment of the deduced protein sequences of the three *Arabidopsis* GGH homologs with that of human GGH (*HsGGH*, GenBank™ NP003869). AtGGH1, 2, and 3 are encoded by genes At1g78660, At1g-78680, and At1g78670, respectively. Identical residues are shaded in *black*, similar residues in *gray*. *Dashes* are gaps introduced to maximize alignment. For the plant sequences, the predicted signal peptide region is *overlined* and potential *N*-glycosylation motifs (N*X*S/T*X*, where *X* is any residue except Pro) are in *red*. *Blue arrowheads* designate conserved residues that are catalytically essential in human GGH, and *black arrowheads* denote other conserved active site residues that may participate in substrate binding. *Dashed underlines* show the three main regions that form the dimer interface in human GGH. *Asterisks* mark the residue of the recombinant proteins to which the His-tag region of the expression vector was fused.

# Supplemental Figure 2

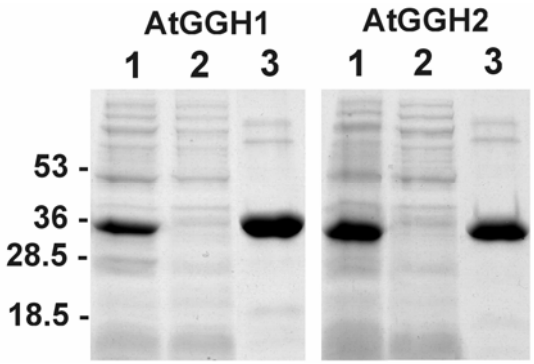


Steps in purification of recombinant AtGGH1 and AtGGH2 proteins. Histidine-tagged AtGGH1 and AtGGH2 were isolated by $Ni^{2+}$ affinity chromatography under native conditions, and separated by SDS-polyacrylamide gel electrophoresis. Gels were stained with Coomassie Blue. For each protein, *lane 1* was loaded with 10 µg of crude *E. coli* extract protein, *lane 2* with 10 µg of the proteins not bound to the resin, and *lane 3* with 5 µg of purified protein. The positions of molecular mass standards (kDa) are indicated.

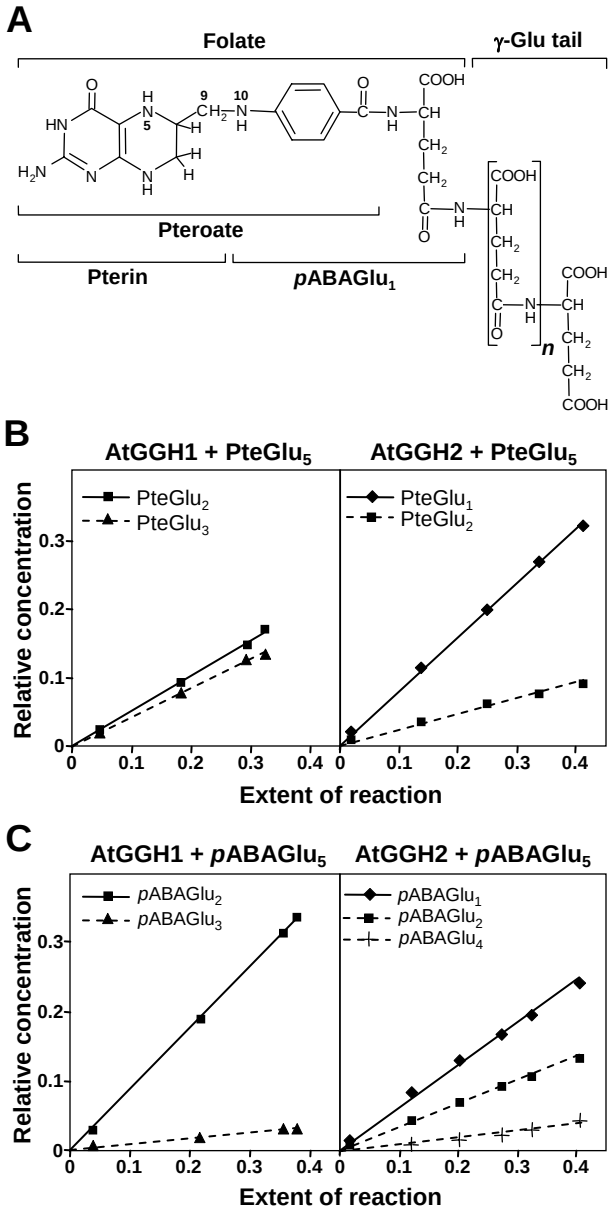


**Fig. 1**

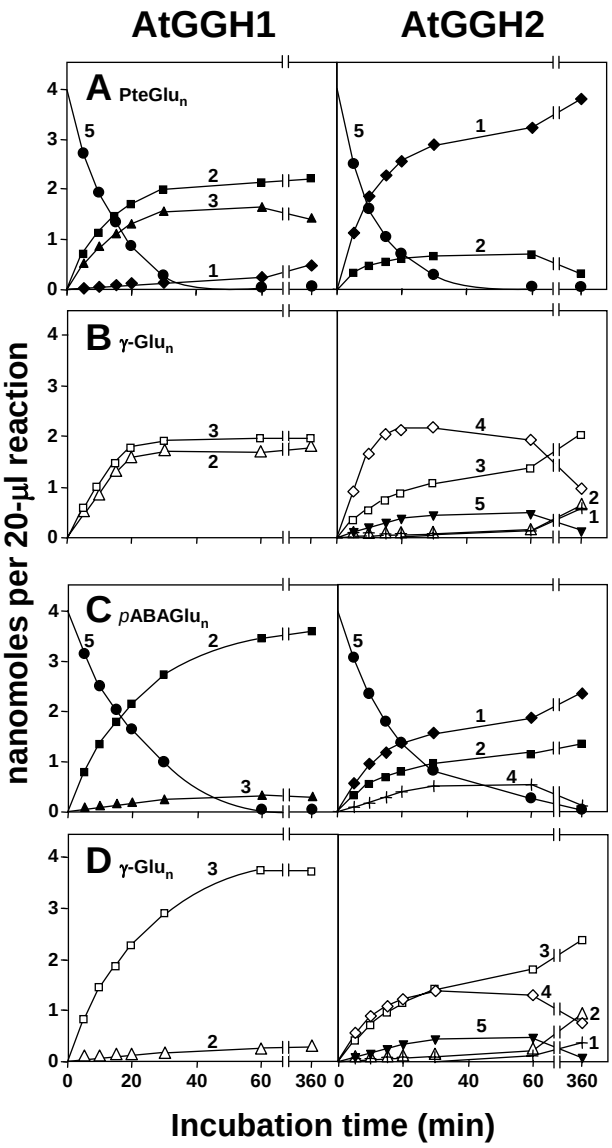


**Fig. 2**

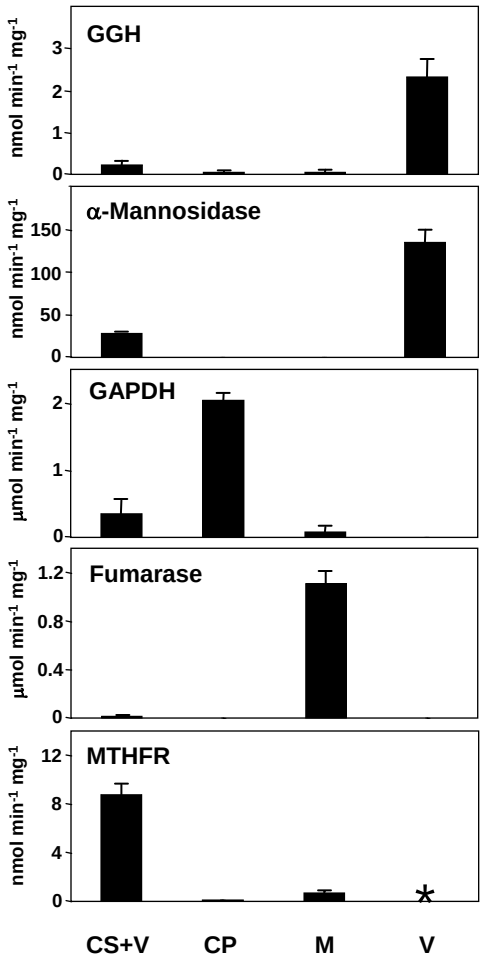


**Fig. 3**

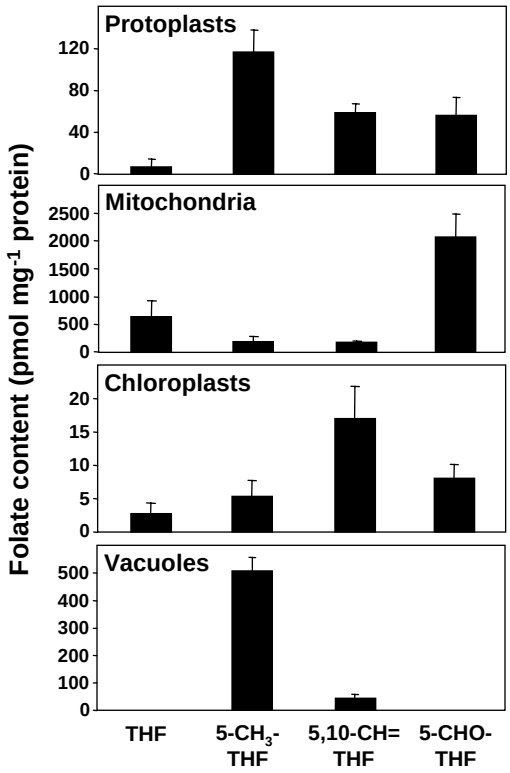


**Fig. 4**

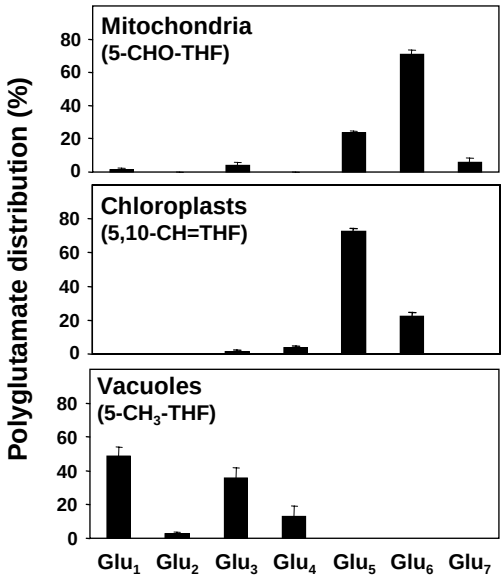


**Fig. 5**

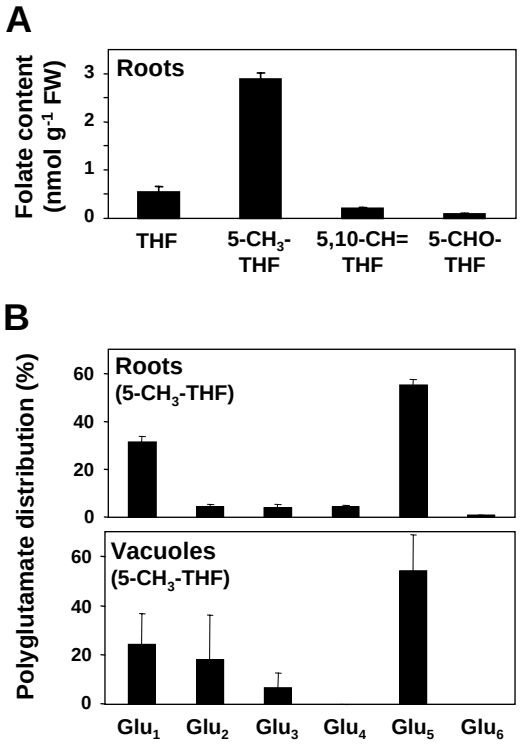


**Fig. 6**

**Plant γ-glutamyl hydrolases and folate polyglutamates: Characterization, compartmentation, and co-occurrence in vacuoles**

Giuseppe Orsomando, Rocio Diaz de la Garza, Brian J. Green, Mingsheng Peng, Philip A. Rea, Thomas J. Ryan, Jesse F. Gregory III and Andrew D. Hanson

*J. Biol. Chem. published online June 16, 2005*

---